Supporting Information

Enhanced Optical Properties of $CsPbX_3$ (X = Cl, Br, and I) Perovskite Nanocrystals Glasses through Bismuth Doping for Light-Emitting Application

Liping Wang,‡[a] Yuqiong Wang,‡[a] Zaiqi Liu,[a] Yu Dong,[a] Puxian Xiong,[c] Chang Xu,*[a] Wen Gao,*[a] and Bo Tang*[a, b]

[a]College of Chemistry, Chemical Engineering and Materials Science, Key Laboratory of Molecular and Nano Probes, Ministry of Education, Collaborative Innovation Center of Functionalized Probes for Chemical Imaging in Universities of Shandong, Institutes of Biomedical Sciences, Shandong Normal University, Jinan 250014, China

[b]Laoshan Laboratory, Qingdao 266237, Shandong, China

[c]State Key Laboratory of Luminescent Materials and Devices, South China University of Technology, Guangzhou, 510641, China

Email address: tangb@sdnu.edu.cn; gaowen@sdnu.edu.cn; 621042@sdnu.edu.cn

Experimental Section

Chemicals

Silicon dioxide (SiO_2, 99%), boron oxide (B_2O_3, 99%), zinc oxide (ZnO, 99%), aluminum oxide (Al_2O_3, 99%), bismuth oxide (Bi_2O_3, 99%), sodium chloride (NaCl, 99%), sodium bromide (NaBr, 99%), sodium iodide (NaI, 99.5%) were purchased from Aladdin Reagent. Cesium carbonate (Cs_2CO_3, 99%), lead chloride ($PbCl_2$, 99.5%), lead bromide ($PbBr_2$, 99%), lead iodide (PbI_2, 98%) were purchased from Macklin Reagent. All chemicals were used without further purification.

Synthesis of Bi_2O_3 doped $CsPbX_3$ glass sample

All glass samples were prepared using traditional melt quenching and subsequent thermal treatment technique. Borosilicate glass was selected as the glass matrix, and NaCl, NaBr, NaI, Cs_2CO_3, $PbCl_2$, $PbBr_2$, PbI_2 were used as precursors to introduce $CsPbX_3$ (X = Cl, Br, I) PNCs into the glass. The raw materials SiO_2, B_2O_3, ZnO, Al_2O_3, Bi_2O_3, NaCl, NaBr, NaI, Cs_2CO_3, $PbCl_2$, $PbBr_2$, PbI_2 were weighed according to the stoichiometric ratio of $mSiO_2$-nB_2O_3-16ZnO-9Al_2O_3-7Cs_2CO_3-14PbX_2-14NaX-xBi_2O_3 (m : n = 1.1 : 1, X = Cl, Br, I; x = 0, 0.05, 0.1, 0.25, 0.5, 0.75, 1.0, 1.5, 2.0, 3.0 mol%). In the following, sample nomenclature is $CsPbX_3$: xBi_2O_3 (X = Cl, Br, I; x = 0, 0.05, 0.10, 0.25, 0.50, 0.75, 1.0, 1.5, 2.0, 3.0 mol%), for instance $CsPbBr_3$: 0.1Bi_2O_3 stands for 20.9SiO_2-19B_2O_3-16ZnO-9Al_2O_3-7Cs_2CO_3-14$PbBr_2$-

14NaBr-0.1Bi_2O_3. All the raw materials were manually mixed and ground to powder in the mortar for 20 min., then the glass powders were transferred to the alumina crucible to stand. The crucible was placed in the heating furnace and melted at 1150 ^oC for 15 minutes. The melts obtained were poured onto a preheated brass mould and then pressed against another steel plate to quench. The quenched glasses were then quickly transferred to a muffle furnace for annealing at 400 ^oC for 4 hours to relieve thermal stress. The prepared glass was then annealed at 480 ^oC for 10 h under air conditions. The $CsPbX_3$ (X = Cl, Br, I) perovskite nanocrystals (PNCs) were gradually grown, and finally the Bi-doped $CsPbX_3$ (X = Cl, Br, I) PNCs glass was successfully prepared by controllable in situ crystallization. All glass samples were cut into ~10×10×1 mm^3 pieces and polished for subsequent optical measurements.

Characterization

The morphology of the sample was observed using a high-resolution transmission electron microscope (TEM, JEM-2100F, JEOL, Japan) operating at 200 kV and equipped with an energy dispersive spectrometry (EDS) detector. Higher magnification TEM images and corresponding elemental distribution was obtained using a spherical aberration electron microscope. The sample utilized for TEM testing finely ground nanoparticles obtained by grinding the block-like glass sample in a mortar. Subsequently, these nanoparticles were further ground for

two hours in an ethyl alcohol solution. The resulting solution was then deposited onto a copper grid for TEM testing. The XRD patterns of the glass samples were determined using an X-ray powder diffractometer (D8 Advance, Bruker, Germany) operating at a scan rate of 10^{o}/min with a step size of 0.02^{o} and a scan range of 5-90^{o}. Fourier transform infrared (FTIR) spectroscopy was used to observe the microstructure of the glass samples using an FTIR spectrometer (Nicolet Magna 750, Madison, USA) with a scanning range of 400-4000 cm^{-1}. Absorption spectra were measured using a UV-VIS spectrophotometer (UV-2600, Shimadzu, Japan) in the absorption mode. X-ray photoelectron spectra (XPS) were recorded using a Thermo Scientific K-Alpha XPS system (Thermo Fisher Scientific Inc., Waltham, UK).

Photoluminescence (PL) spectra, excitation spectra were recorded using a spectrophotometer (FLS1000, Edinburgh Instruments, UK) equipped with a 450 W xenon lamp. Fluorescence decay curves were monitored using fluorescence lifetime spectrometer (Hamamatsu Photonics Quantaurus-Tau C16361-2). The temperature dependent PL spectra were monitored using the same spectrophotometer connected to a self-regulating heater. Photoluminescence quantum yields (PLQYs) were measured using the same fluorescence spectrometer equipped with a barium sulfate coated integrating sphere. The green LED and the red LED were fabricated by coating Bi-doped $CsPbBr_3$ PNCs glasses and Bi-doped $CsPbI_3$ PNCs glasses based on InGaN chips, respectively.

Colour rendering index (CRI), correlated colour temperature (CCT), luminous efficiency (LE), and Commission Internationale de L'Eclairage (CIE) coordinates of the green LED and the red LED were recorded using an integrated sphere spectroradiometer (HAAS-2000, Everfine, China) under a current of 20 mA. The electroluminescence (EL) properties of the fabricated LEDs were measured using the USB 4000 fiber optic spectrometer (Ocean Optics).

In the fluorescence imaging application, the green emission LED device were prepared and successfully used for fluorescence probe imaging. As illustrated in Fig. S16, a green emission LED was fabricated using a Bi-doped $CsPbBr_3$ PNCs glass package. The block-shaped Bi-doped $CsPbBr_3$ PNCs glass was affixed to the surface of the blue LED chip (wavelength: 465 nm) and secured by four small screws. The Bi-doped $CsPbBr_3$ based LED light source exhibited better focusing ability by covering the reflector cup and convex lens on the glass samples surface. To prevent the accumulation of thermal energy, the device was also equipped with an LED heat sink for thermal dissipation. A miniaturized and portable fluorescence detection device was successfully constructed as shown in Fig. 5k.

Supporting Figures and Tables

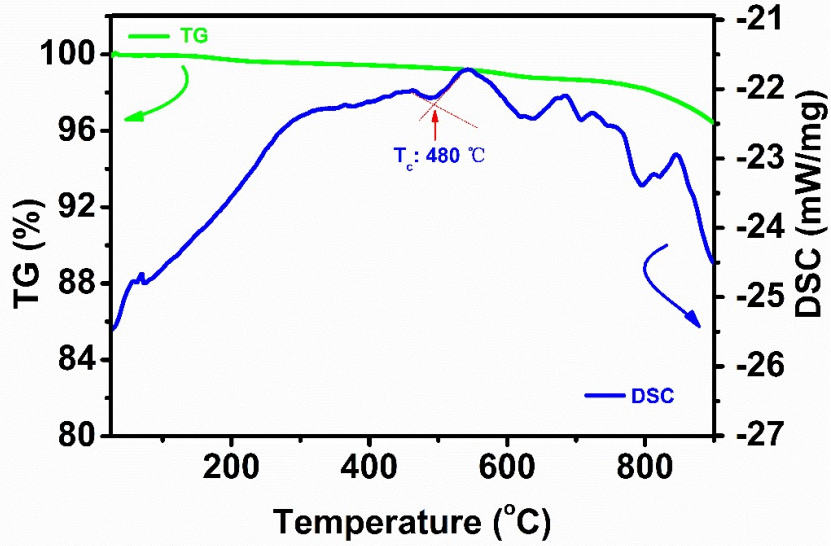

Fig. S1 TG-DSC curves of the representative $CsPbI_3$: $0.5Bi_2O_3$ PNCs glass samples

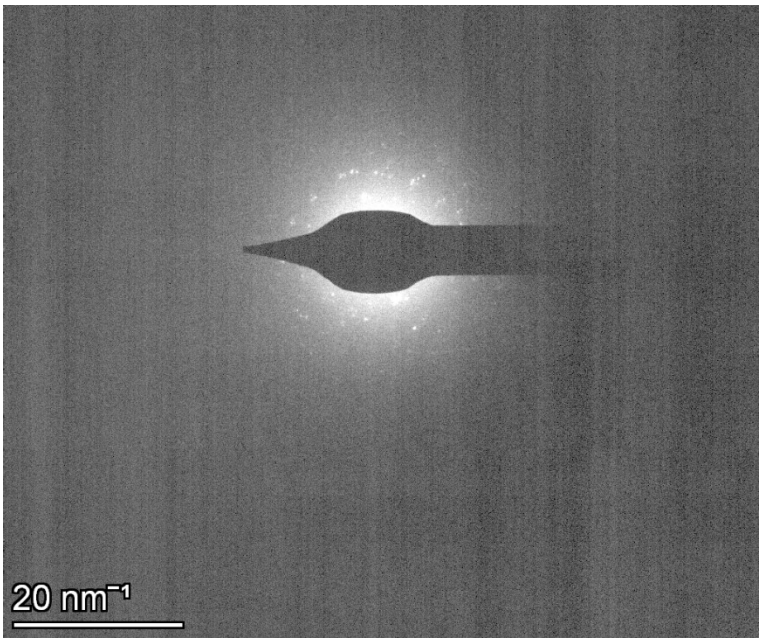

Fig. S2 Selected area electron diffraction patterns of $CsPbCl_3$: 0.5 Bi_2O_3 PNCs glass samples

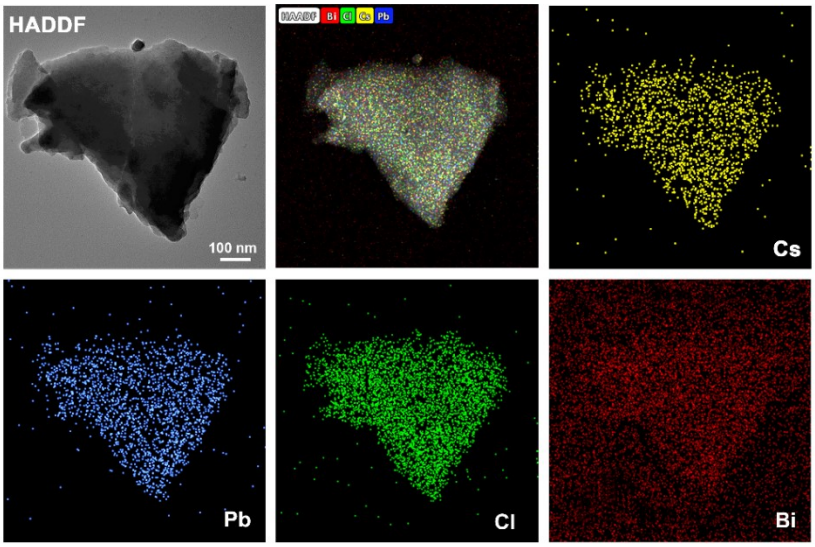

Fig. S3 EDS elemental mapping of $CsPbCl_3$: $0.5Bi_2O_3$ PNCs glass samples.

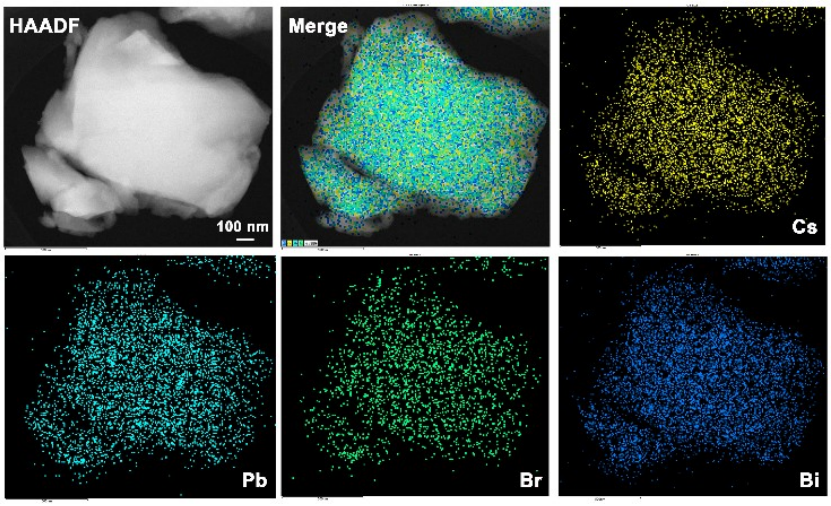

Fig. S4 EDS elemental mapping of $CsPbBr_3$: $0.5Bi_2O_3$ PNCs glass samples.

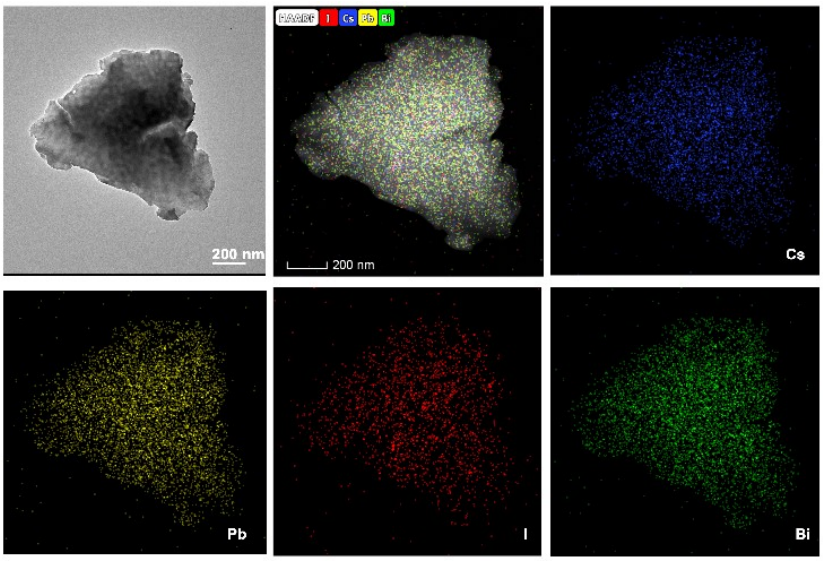

Fig. S5 EDS elemental mapping of $CsPbI_3$: $0.5Bi_2O_3$ PNCs glass samples.

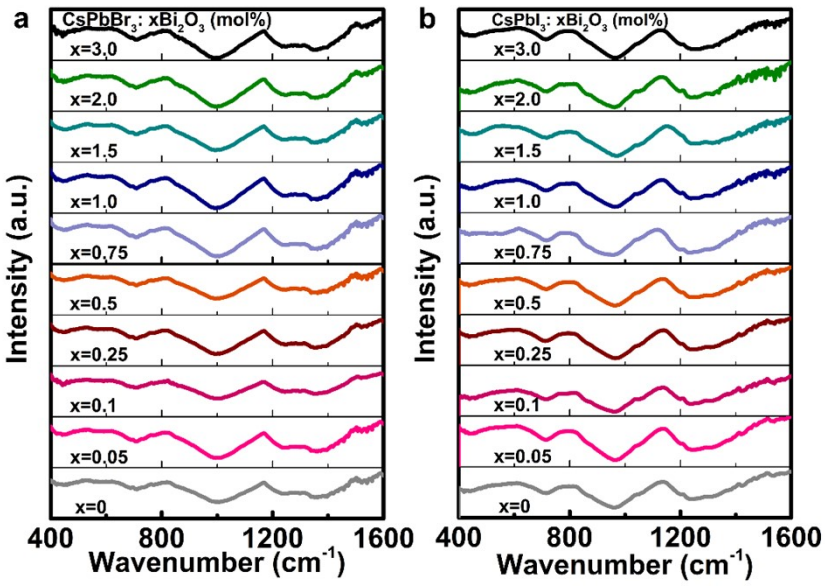

Fig. S6 FTIR spectra of $CsPbBr_3$: xBi_2O_3 and $CsPbI_3$: xBi_2O_3 (x = 0, 0.05, 0.10, 0.25, 0.50, 0.75, 1.0, 1.5, 2.0, 3.0 mol%) PNCs glass samples.

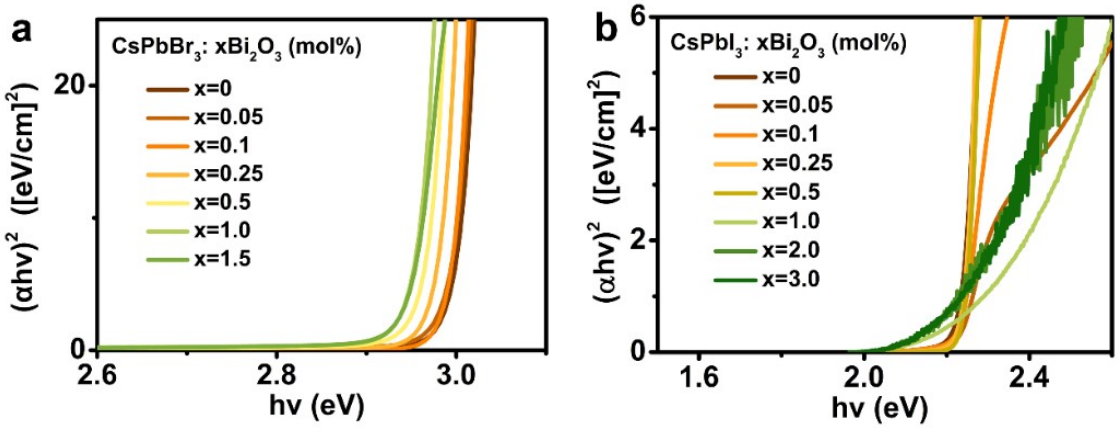

Fig. S7 The dependence of $(\alpha hu)^2$ vs. hu for $CsPbBr_3$: xBi_2O_3 and $CsPbI_3$: xBi_2O_3 (x = 0, 0.05, 0.1, 0.25, 0.5, 0.75, 1.0, 1.5 mol%) PNCs glasses.

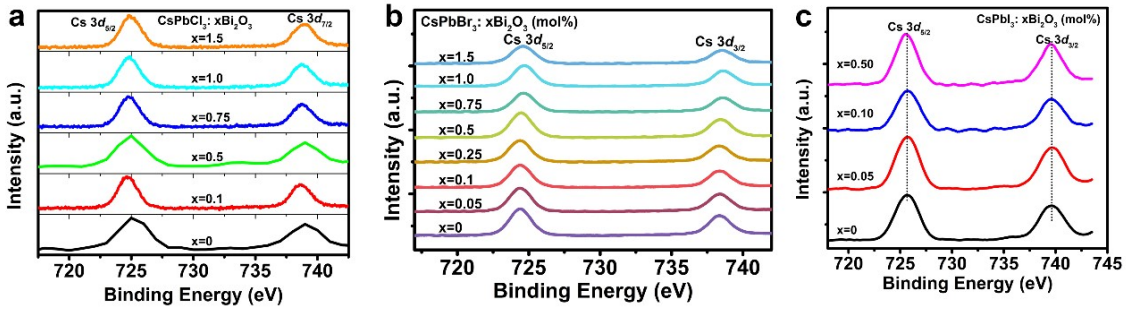

Fig. S8 High-resolution XPS spectra of Cs 3d from (a) $CsPbCl_3$: xBi_2O_3, (b) $CsPbBr_3$: xBi_2O_3, (c) $CsPbI_3$: xBi_2O_3 (x = 0, 0.05, 0.10, 0.25, 0.50, 0.75, 1.0, 1.5 mol%) PNCs glass samples, respectively.

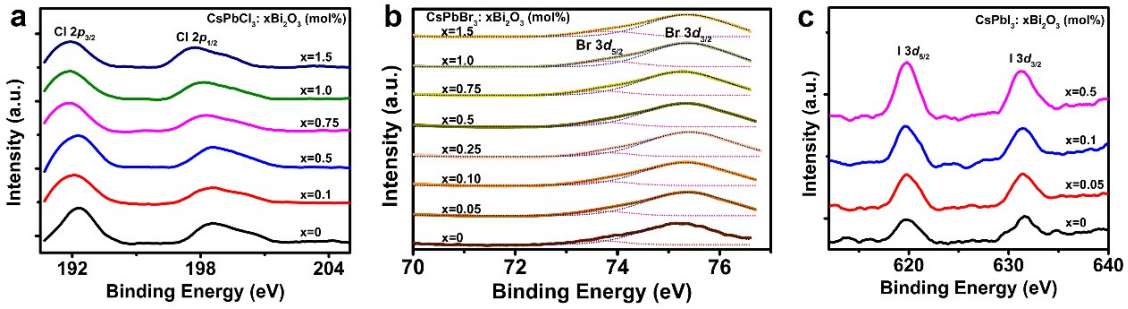

Fig. S9 High-resolution XPS spectra of (a) Cl 2p, (b) Br 3d and (c) I 3d regions.

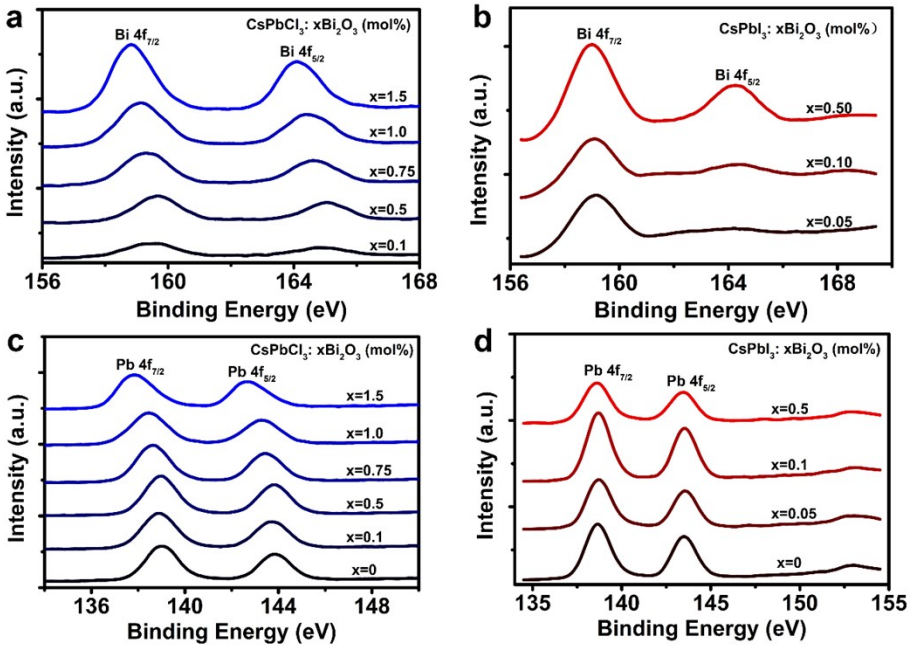

Fig. S10 High-resolution XPS spectra of (a, b) Bi *2p* and (c, d) Pb *4f* regions from the $CsPbCl_3$: xBi_2O_3 (x = 0, 0.1, 0.5, 0.75, 1.0, 1.5 mol%) and (b) $CsPbI_3$: xBi_2O_3 (x = 0, 0.05, 0.10, 0.50 mol%) PNCs glass samples.

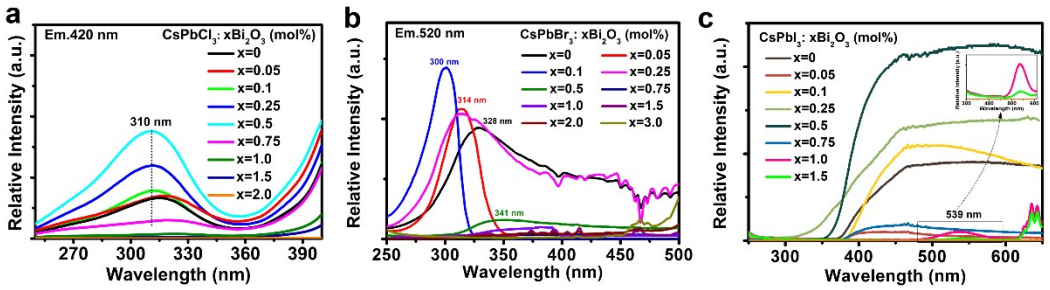

Fig. S11 Excitation spectra of (a) $CsPbCl_3$: xBi_2O_3 monitored at 420 nm, (b) $CsPbBr_3$: xBi_2O_3 PNCs glass samples monitored at 520 nm and (c) $CsPbI_3$: xBi_2O_3 monitored at 700 nm.

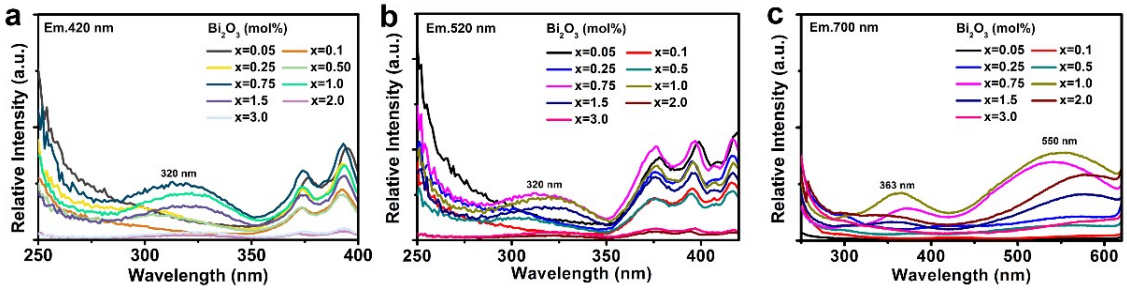

Fig. S12 Excitation spectra of Bi_2O_3 doped borosilicate glasses (x = 0.05, 0.10, 0.25, 0.50, 0.75, 1.0, 1.5, 2.0, 3.0 mol%) without introducing $CsPbX_3$ (X = Cl, Br, I) PNCs glass samples monitored at (a) 420 nm, (b) 520 nm and (c) 700 nm, respectively.

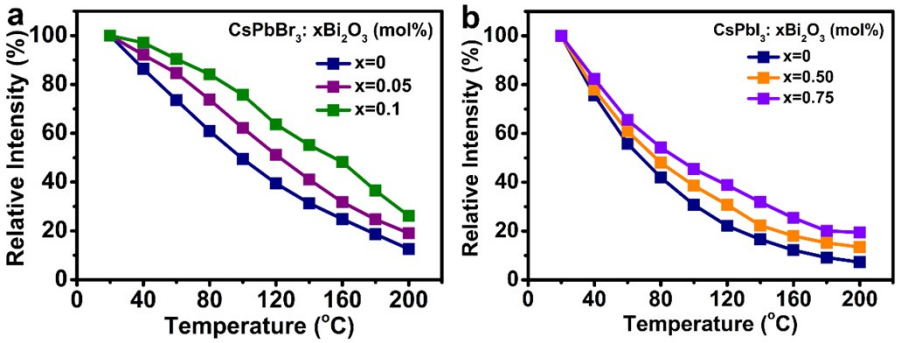

Fig. S13 Temperature-dependent PL intensities for (a) $CsPbBr_3$: xBi_2O_3 (x = 0, 0.05, 0.10) PNCs glass samples and $CsPbI_3$: xBi_2O_3 PNCs glass samples (x = 0, 0.50, 0.75 mol%) via heating at 20-200 °C.

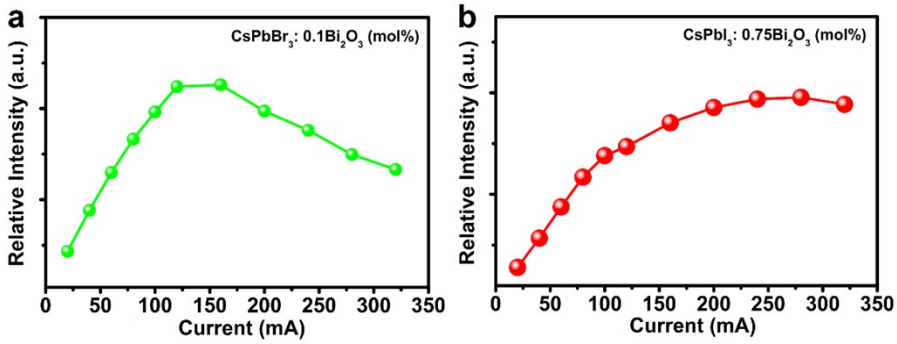

Fig. S14 Current-dependent EL intensities for (a) $CsPbBr_3$: $0.1Bi_2O_3$ PNCs glass samples and $CsPbI_3$: $0.75Bi_2O_3$ PNCs glass samples.

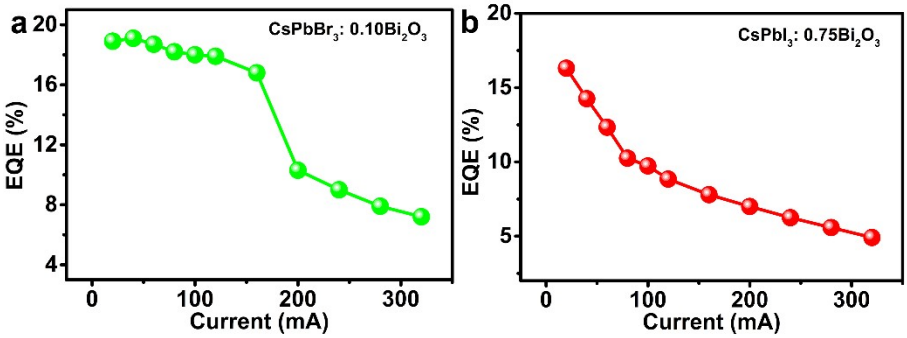

Fig. S15 Current-dependent external quantum efficiency (EQE) for (a) $CsPbBr_3$: $0.1Bi_2O_3$ PNCs glass samples and $CsPbI_3$: $0.75Bi_2O_3$ PNCs glass samples.

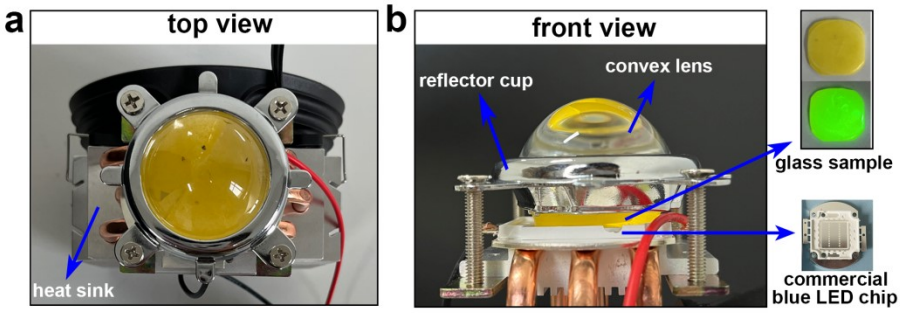

Fig. S16 The images of a green LED obtained by the encapsulation of Bi-doped $CsPbBr_3$ PNCs glass. (a) Top view, (b) Front view

Table S1. Absorption bandgaps of Bi doped $CsPbX_3$ (X = Cl, Br, I) PNCs glass samples (0-1.5 mol%) obtained by extrapolation to $(\alpha h\upsilon)^2 = 0$.

Bi_2O_3 (x, mol%)	Bandgap (eV)		
	$CsPbCl_3$: xBi_2O_3	$CsPbBr_3$: xBi_2O_3	$CsPbI_3$: xBi_2O_3
0	4.60	3.02	2.23
0.05	4.59	3.01	2.24
0.10	4.56	3.0	2.24
0.25	4.55	2.99	2.24
0.50	4.36	2.98	2.24
0.75	4.47	2.95	2.26
1.0	4.41	2.96	2.28
1.5	4.39	2.97	